Silica particle characterization

The size distributions of the silica particles were measured with a Zetasizer 3000HS (Worcestershire, United Kingdom) after sonication of the particles at a concentration of 300 μg/mL in H_2O.

Cytotoxicity assay and cytokine production assay

RAW264.7 cells (1.5×10^4 cells/well) were seeded in 96-well plates (Nunc, Rochester, NY), cultured at 37°C for 12 h, and then treated with each type of silica particle (100 μg/mL) or medium (for negative control) for 12 h. The cytotoxicity of the silica particles was assessed by means of the standard methylene blue assay method, as previously described (Morishige et al. 2010a). Production of tumor necrosis factor-α (TNFα) in culture supernatants was assessed by means of an enzyme-linked immunosorbent assay (ELISA) kit (BD Pharmingen, San Diego, CA) according to the manufacturer's instructions.

Inhibitory assay

RAW264.7 cells (1.5×10^4 cells/well) were seeded in 96-well plates (Nunc), cultured at 37°C for 12 h, and then preincubated for 2 h with SB203580 (50 μM), U0126 (50 μM), SP600125 (10 μM), BHA (50 or 250 μM), or DPI (2 or 10 μM). Then, the cells were treated with one type of silica particle (100 μg/mL) or medium (for negative control) for 4 h. TNFα production in the culture supernatants was assessed by means of an ELISA kit (BD Pharmingen) according to the manufacturer's instructions.

Western blotting analysis

RAW264.7 cells were seeded in 12-well plates, cultured at 37°C for 12 h, and then treated with one type of silica particle (100 μg/mL) or medium (for negative control) for 0.5, 1, 2, or 4 h. For positive control, cells were treated with lipopolysaccharide (LPS) (1.25 μg/mL) for 30 min. Cells were then washed with PBS and lysed with Mammalian Protein Extraction Reagent (M-PER; Thermo Fisher Scientific, Rockford, IL) containing a Halt Protease Inhibitor Cocktail Kit (Thermo Fisher Scientific) and Phosphatase Inhibitor Cocktail (Nacalai Tesque, Kyoto, Japan). Then protein samples (1–5 μg) were loaded on a 20% sodium dodecyl sulfate–polyacrylamide gel. After electrophoresis, proteins were transferred to polyvinylidene difluoride membranes (GE Healthcare, Buckinghamshire, United Kingdom). The blots were blocked with 4% ECL Advance Blocking Agent (GE Healthcare) in TBS/T buffer (20 mM Tris–HCl [pH 7.6], 137 mM NaCl, 0.1% Tween 20) for 2 h at room temperature. The blots were washed with TBS/T and incubated with primary antibodies overnight at 4°C. Goat anti-rabbit or goat anti-mouse peroxidase-conjugated secondary antibody was added to the membranes, which were then incubated for 1 h at room temperature. The protein bands on the membrane were visualized with SuperSignal West Femto Maximum Sensitivity Substrate (Thermo Fisher Scientific).

Transmission electron microscopy (TEM) analysis

RAW264.7 cells (3×10^5 cells/well) were seeded in 4-well Lab-Tek II Chambered Coverglass (Nunc), cultured at 37°C for 6 h, treated with 100 μg/mL nSP70, nSP70-C or medium (for negative control), and fixed in 2.5% glutaraldehyde and then in 1.5% osmium tetraoxide. The fixed cells were dehydrated and embedded in EPON resin. Ultrathin sections were stained with lead citrate and observed by transmission electron microscopy (HITACHI-H7650, HITACHI, Tokyo, Japan).

Assessment of in vivo inflammatory effects of silica particles

BALB/c mice were intraperitoneally injected with 1 mg of one type of silica particle in 200 μL phosphate-buffered saline (PBS) or PBS for negative control. Two or twenty-four hours after injection, the mice were sacrificed, and whole peritoneal cavity lavage fluid (PCLF) was collected using 4 mL of cooled PBS as previously described (Kops et al. 1986; Morishige et al. 2010a). Cytokine production patterns in the PCLF 2 h after injection were analyzed by means of a Mouse Cytokine 20-Plex Panel (Invitrogen, Carlsbad, CA) using a Bio-Plex Suspension Array System (Bio-Rad Laboratories, Tokyo, Japan). The total number of live cells in the PCLF 24 h after injection was determined with a Nucleo-Counter (Chemometec A/S, Allerød, Denmark).

Statistical analysis

All results are presented as means ± standard deviation (SD) or standard error of the mean (SEM). Differences were compared by using Student's *t*-tests or Scheffé's method after analysis of variance (ANOVA).

Results

Size dependence of silica particle-induced inflammatory responses

Here, we used nanosilica particles with diameters of 30 and 70 nm (nSP30 and nSP70, respectively) and conventional

microsilica particles with diameters of 300 and 1,000 nm (nSP300 and mSP1000, respectively). The hydrodynamic diameters of these particles, as measured by means of a dynamic light-scattering system, were 33, 78, 300, and 945 nm, respectively (Fig. 1a). The size distribution spectrum of each silica particle showed a single peak (Fig. 1a), and the hydrodynamic diameter corresponded almost precisely to the primary particle size for each sample, indicating that the silica particles used in this study were well-dispersed particles in solution. In addition, TEM images confirmed that the particles were well-dispersed smooth-surfaced spheres, as described previously (Yamashita et al. 2011). First, we assessed the correlation between the size of the silica particles and their inflammatory effects. We incubated RAW264.7 cells with each type of silica particle and measured TNFα production in the culture supernatant, because TNFα is a crucial modulator of inflammation (Fig. 1b). Of the various silica particles, nSP30 and nSP70 induced the highest TNFα production, whereas the larger nSP300 and mSP1000 did not induce such inflammatory responses.

Next, we assessed the correlation between particle size and inflammatory effects in vivo (Fig. 1c, d). We intraperitoneally injected silica particles into BALB/c mice and counted the total number of live cells in the PCLF, because inflammation is known to induce local infiltration of various inflammatory cells (Busuttil et al. 2004). We found that nSP30 and nSP70 induced significant cell migration compared with PBS, whereas nSP300 and mSP1000 showed low cell accumulation (Fig. 1c). Furthermore, we analyzed cytokine and chemokine production in the PCLF by using a cytokine array system (Fig. 1d). nSP30 and nSP70 induced greater production of interleukin-5 (IL-5) and IL-6, macrophage chemoattractant protein-1 (MCP-1), and keratinocyte chemoattractant (KC) than did nSP300 and mSP1000, although TNFα production was not detected in the PCLF. These results indicate that the nanosilica particles possessed a more potent inflammatory effect than did the larger silica particles.

Involvement of mitogen-activated protein kinases in nanosilica particle-induced inflammation

Mitogen-activated protein kinases (MAPKs) are a family of proteins, including p38, ERK, and JNK, that play key roles in regulation of the production of proinflammatory mediators and in apoptotic cell death (Jeffrey et al. 2007). To investigate the mechanisms of nanosilica particle-induced inflammation, we treated RAW264.7 cells with silica particles and used Western blotting analysis to examine the activation of MAPKs (Fig. 2a–c). We detected the phosphorylation of p38, ERK, and JNK in nSP30- and nSP70-treated cells. In contrast, little or no phosphorylation of

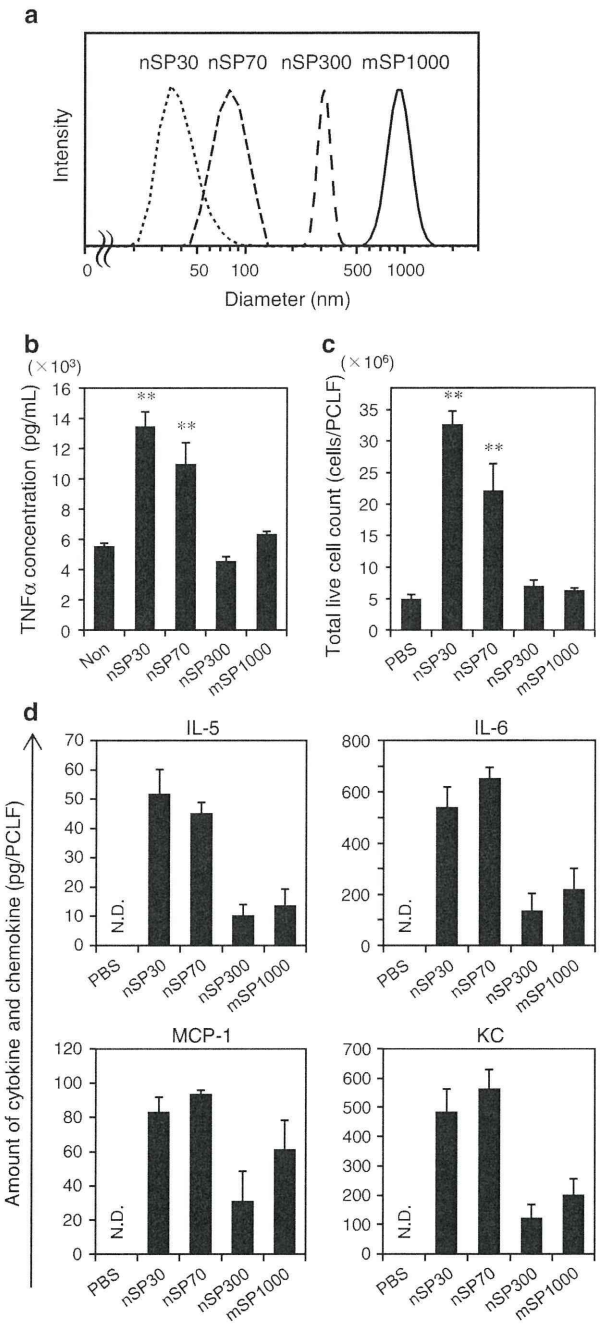

Fig. 1 Correlation between silica particle size and inflammatory effects in vitro and in vivo. **a** Size distribution of various sizes of silica particles was measured by a dynamic light-scattering method. **b** TNFα production levels in vitro. RAW264.7 cells were treated with each silica particle or no particles (Non) for 12 h, and then, TNFα production levels in the culture supernatants were measured. The data represent means ± SD ($n = 5$; $^{**}P < 0.01$ versus value for medium control, ANOVA). **c**, **d** In vivo inflammatory effects. BALB/c mice were intraperitoneally injected with PBS or each silica particle; then, **c** the total number of live cells in the PCLF was counted after 24 h, and **d** cytokine and chemokine production in the PCLF was measured after 2 h. *N.D.* not detected. Data represent means ± SEM ($n = 5$; $^{**}P < 0.01$ versus value for PBS control, ANOVA)

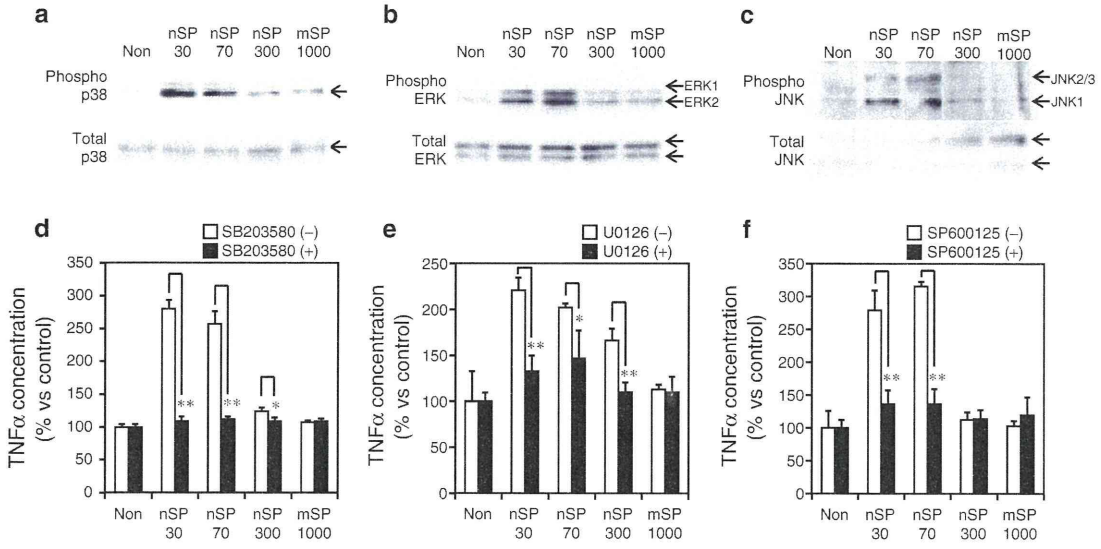

Fig. 2 Effects of silica particles on the activation of MAPKs. **a–c** Activation of MAPKs induced by silica particles. RAW264.7 cells were treated with silica particles of various sizes for 4 h. The whole-cell lysates were analyzed by Western blotting for phosphorylated and nonphosphorylated **a** p38, **b** ERK, and **c** JNK. **d–f** Association of MAPKs in silica particle-induced TNFα production. RAW264.7 cells, pretreated with inhibitors of **d** p38, **e** ERK, or **f** JNK were exposed to silica particles, and 4 h after the treatment, TNFα production in the culture supernatants was measured. Dimethyl sulfoxide (0.1%) was used as the control. Data represent means ± SD ($n = 5$; $^{*}P < 0.05$, $^{**}P < 0.01$ versus value for inhibitor [–] control within each treatment pair, t test)

MAPKs was detected in cells treated with nSP300 or mSP1000. No changes in the expression of nonphosphorylated p38, ERK, and JNK were observed in cells treated with silica particles. These results suggest that nanosilica particles might have induced inflammation via activation of MAPKs.

To confirm the importance of MAPKs in nanosilica particle-induced inflammation, we analyzed TNFα production in RAW264.7 cells treated with silica particles in the presence of an inhibitor of p38 (SB203580), ERK (U0126), or JNK (SP600125) (Fig. 2d–f). nSP30- and nSP70-induced TNFα production was almost completely suppressed by the inhibitors, indicating that nanosilica particle-induced TNFα production was mediated by MAPKs. Taken together, these results indicate that significant nanosilica particle-induced inflammation was mediated by the activation of MAPKs, whereas microsilica particles had little activation effect on MAPKs.

Involvement of the production of reactive oxygen species in nanosilica particle-induced inflammation

Intracellular reactive oxygen species (ROS) are reported to function as second messengers of inflammatory effects by activating multiple signaling pathways including a series of MAPKs (Bubici et al. 2006; Thannickal and Fanburg 2000). To investigate the involvement of ROS in nanosilica particle-induced TNFα production, we measured the TNFα concentrations induced by nSP30 and nSP70 in the presence BHA, a broad-spectrum ROS scavenger, or DPI, a specific inhibitor of NADPH oxidase, which is an important enzymatic producer of ROS (Morel et al. 1991). Both BHA and DPI significantly suppressed nanosilica particle-induced TNFα production (Fig. 3a, b), suggesting that nanosilica particle-induced production of ROS plays an important role in MAPK activation and subsequent inflammatory responses.

Suppression of inflammation by surface modification of nSP70

To investigate the influence of surface modification on nanosilica particle-induced inflammatory responses, we used nSP70 of which the surfaces had been modified with COOH groups (nSP70-C). We confirmed that nSP70-C were smooth-surfaced spherical particles by TEM as described previously (Yamashita et al. 2011). The mean secondary particle diameter of the nSP70-C was 70 nm, and the zeta potentials of nSP70 and nSP70-C were −53 and −76, respectively, indicating that surface modification changed the surface charge of the particles as described previously (Yamashita et al. 2011). We incubated RAW264.7 cells with nSP70 or nSP70-C for 12 h and then measured the TNFα concentrations. Whereas nSP70 induced high levels of TNFα production, nSP70-C induced low levels of TNFα production (Fig. 4a). Furthermore, we evaluated the inflammatory effects of nSP70 and nSP70-C in vivo. We intraperitoneally injected both types of particle separately into BALB/c mice

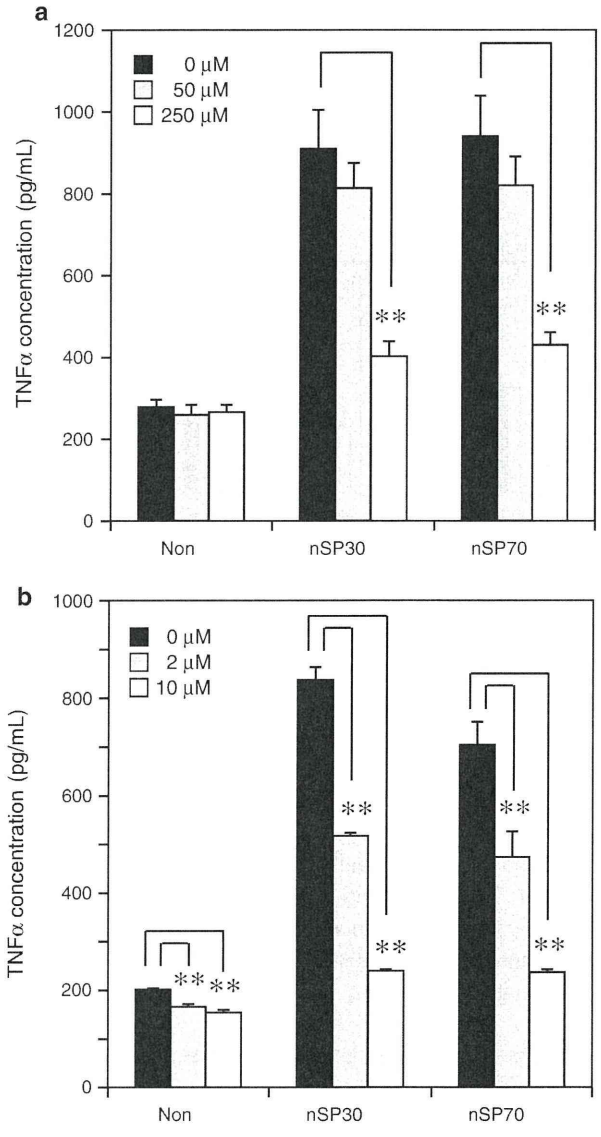

Fig. 3 Involvement of nanosilica particle-induced ROS production in TNFα production. RAW264.7 cells were treated with nSP30 or nSP70 for 4 h in the absence or presence of **a** BHA or **b** DPI at the indicated concentrations. TNFα production in the culture supernatants was measured. Data represent means ± SD ($n = 5$; $^{**}P < 0.01$ versus value for inhibitor [−] control within each treatment pair, *t* test)

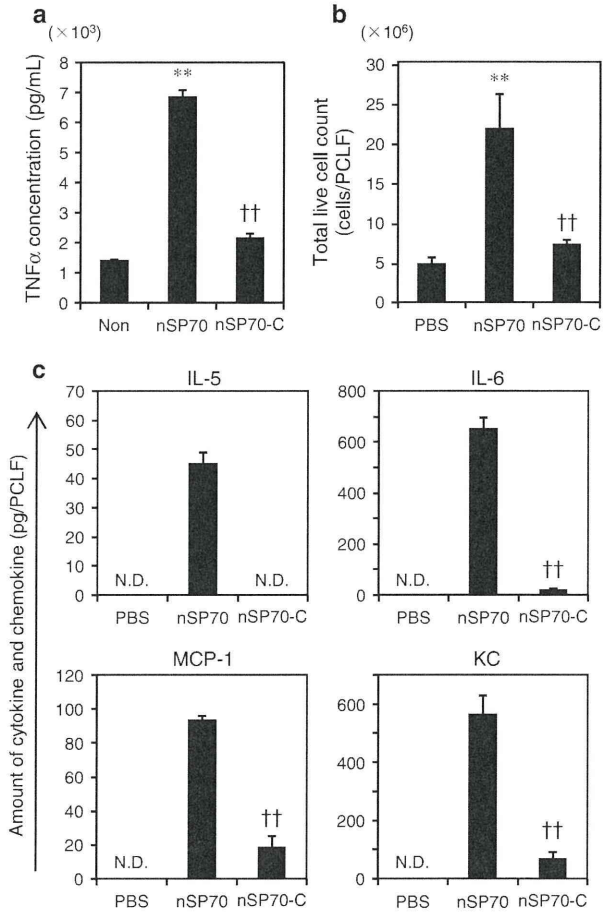

Fig. 4 Inflammatory responses induced by surface-modified nSP70. **a** TNFα production induced by nSP70 and nSP70-C. RAW264.7 cells were treated with nSP70 or nSP70-C for 12 h, and then, TNFα production in the culture supernatants was measured. Data represent means ± SD ($n = 5$; $^{**}P < 0.01$ versus value for medium control, $^{\dagger\dagger}P < 0.01$ versus value for nSP70, ANOVA). **b**, **c** In vivo inflammatory effects of nSP70 and nSP70-C. BALB/c mice were intraperitoneally injected with PBS or nSP70 or nSP70-C; **b** the total number of live cells in the PCLF was counted after 24 h, and **c** cytokine and chemokine production in the PCLF was measured after 2 h. *N.D.* not detected. Data represent means ± SEM ($n = 5$; $^{**}P < 0.01$ versus value for PBS control, $^{\dagger\dagger}P < 0.01$ versus value for nSP70, ANOVA)

and then counted the total number of live cells and measured the production of cytokines and chemokines in the PCLF. nSP70-C did not induce significant cell migration in treated mice, even though nSP70 induced strong inflammatory responses (Fig. 4b). In addition, cytokine and chemokine production in nSP70-C-treated mice was significantly lower than in nSP70-treated mice (Fig. 4c). We also confirmed that, in the 20-plex cytokine array system used in this study, there was no upregulation of cytokine and chemokine production in the nSP70-C-treated group (data not shown). These results indicate that nSP70 modified with COOH groups are unlikely to induce undesired inflammatory responses.

Suppression of MAPK activation by surface modification of nSP70

Through their phagocytic activity, macrophages play an important role in determining the biopersistence of foreign particles and initiating inflammatory responses, including cytokine production. Therefore, we speculated that the reduction of inflammatory responses by surface modification of nSP70 resulted from a difference in the particle

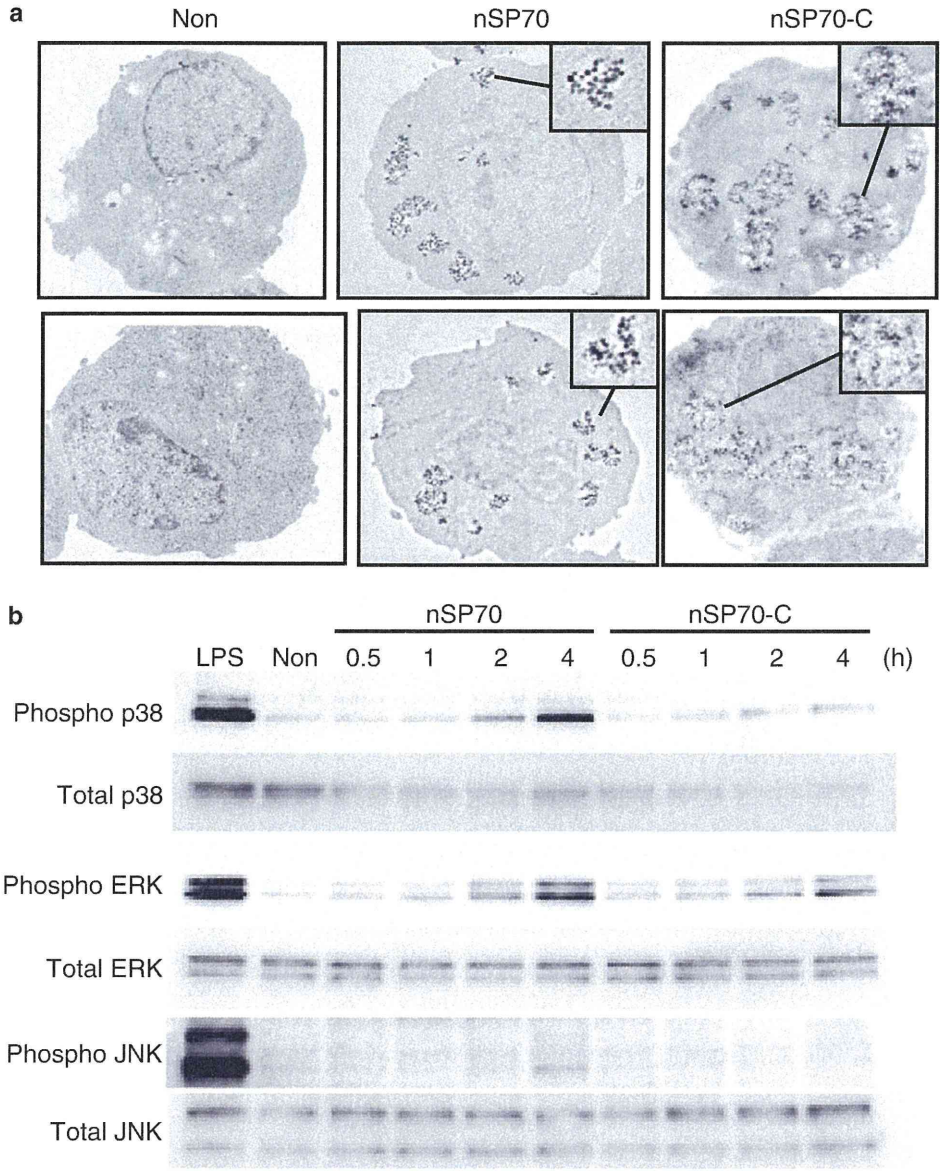

Fig. 5 Effects of surface modification of nSP70 on the MAPKs pathway. **a** TEM analysis of nSP70 and nSP70-C. RAW264.7 cells were treated with nSP70 or nSP70-C for 4 h. Cells were then observed by TEM. **b** MAPK activation induced by nSP70 or nSP70-C. RAW264.7 cells were treated with nSP70 or nSP70-C for the indicated times. The whole-cell lysate was analyzed by Western blotting for phosphorylated and nonphosphorylated p38, ERK, and JNK

uptake frequency between the modified and unmodified nSP70. TEM analysis of the uptake frequency of nSP70-C clearly showed that they were taken up by RAW264.7 cells as well as nSP70 (Fig. 5a). Therefore, we attributed the difference between the inflammatory effects of the modified and unmodified particles to a difference in signaling intensity after ingestion of the particles into the cells. To elucidate the mechanisms by which surface modification suppressed the inflammatory effect of nSP70, we examined the activity of MAPKs in RAW264.7 cells treated with modified or unmodified nSP70 (Fig. 5b). nSP70-C induced low MAPK activation compared with nSP70 4 h after the treatment, although there was no noticeable difference at the time point of 0.5, 1, and 2 h after the treatment. Taken together, our observations suggest that surface modification of nSP70 suppressed TNFα production by reducing nSP70-induced MAPK activation rather than by reducing cellular uptake frequency.

Cytotoxicity of silica particles

MAPKs are associated with cell growth, cell differentiation, and apoptotic cell death (Shiryaev and Moens 2010). Therefore, to investigate the influence of silica particle size on cytotoxicity, we treated RAW264.7 cells with silica particles of various sizes and examined the cell viability. nSP30 and nSP70 had significant cytotoxicity compared with the larger particles (nSP300 and mSP1000; Fig. 6a). To determine the impact of surface modification of the silica particles on cytotoxicity, we incubated RAW264.7

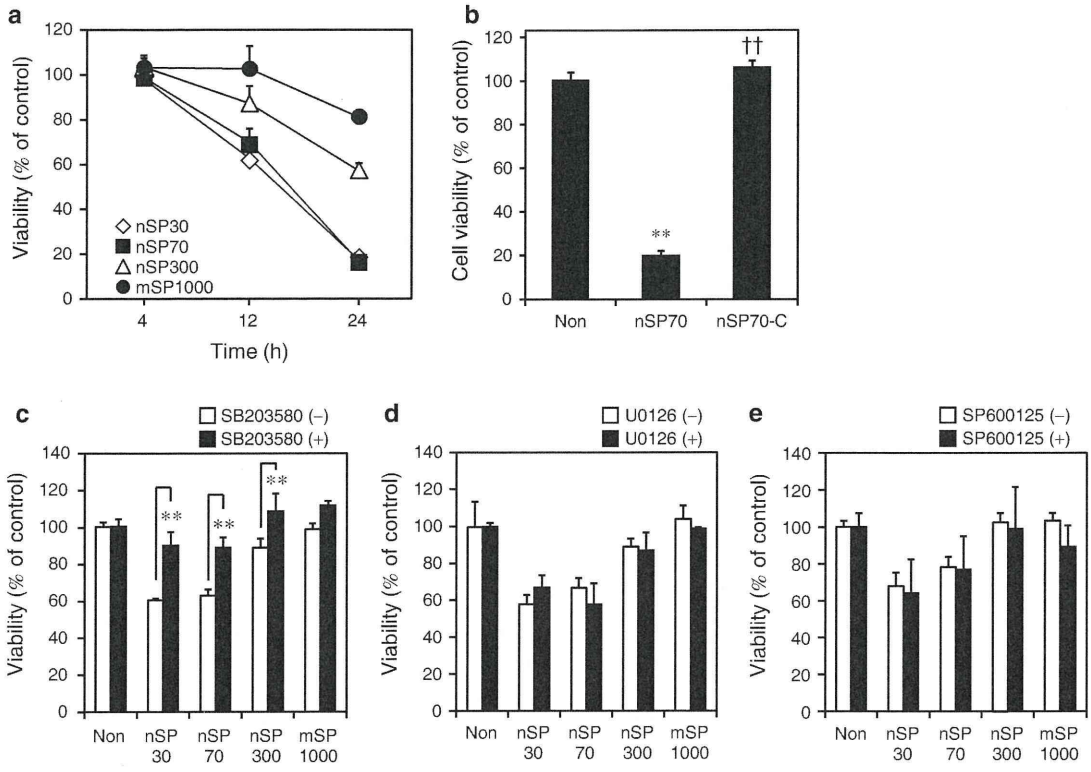

Fig. 6 Cytotoxicity induced by silica particles. **a** Cytotoxicity of silica particles. RAW264.7 cells were treated with silica particles of various sizes for the indicated time. Cell viability was assessed. Data represent means ± SD ($n = 5$). **b** Cytotoxicity of nSP70-C. RAW264.7 cells were treated with nSP70 or nSP70-C for 24 h. Cell viability was assessed. Data represent means ± SD ($n = 5$; $^{**}P < 0.01$ versus value for medium control, $^{\dagger\dagger}P < 0.01$ versus value for nSP70, ANOVA). **c–e** Association of MAPKs with silica particle-induced cell death. RAW264.7 cells pretreated with inhibitors of **c** p38 MAPK, **d** ERK, or **e** JNK were exposed to silica particles, and 12 h after the treatment, cell viability was assessed. Dimethyl sulfoxide (0.1%) was used as a control. Data represent means ± SD ($n = 5$; $^{**}P < 0.01$ versus value for inhibitor [–] control within each treatment pair, t test)

cells with nSP70 and nSP70-C and again evaluated the cell viability. nSP70-C showed no cytotoxicity, whereas nSP70 induced significant cell death (Fig. 6b). We speculated that nanosilica particle-induced cell death depended on MAPK signaling triggered by nanosilica particles. Therefore, to investigate the association of MAPKs and nanosilica particle-induced cell death, we treated RAW264.7 cells with silica particles in the presence or absence of an inhibitor of p38 (SB203580), ERK (U0126), or JNK (SP600125). The p38 inhibitor (SB203580) significantly suppressed the cytotoxicity of nanosilica particles (Fig. 6c–e), whereas the inhibitors of ERK (U0126) and JNK (SP600125) did not. These findings indicate that nanosilica particle-induced cell death depended in part on p38, but was independent of ERK and JNK.

Discussion

We elucidated the effects of particle size and surface modification on silica particle-induced inflammatory responses, with the goal of obtaining basic information for use in the development of safe and effective nanomaterials. First, we evaluated the association between the size of silica particles and their inflammatory effects. We focused on TNFα production, because TNFα stimulates the acute-phase reaction and is involved in systemic inflammation. Furthermore, recent reports have shown that TNFα plays a critical role in the pathogenesis of silicosis (Li et al. 2009). We showed that nSP30 and nSP70 induced significant TNFα production in vitro, whereas nSP300 and mSP1000 exhibited low levels of TNFα production (Fig. 1b). In addition, we demonstrated that the nSP30 and nSP70 induced higher in vivo inflammatory responses than did nSP300 and mSP1000 (Fig. 1c, d). Among the most important sources of cytokines against inhaled foreign particles are macrophages, which are widely known as the first line of defense against such particles (Hornung et al. 2008). We attributed nanosilica particle-induced cytokine production to the inflammatory signaling cascade triggered by ingestion of the nanosilica particles by macrophages. Consistent with our consideration, the results obtained by

other studies indicate that smaller titanium dioxide particles induce strong inflammatory responses than do larger particles (Sager et al. 2008). Therefore, we suggest that investigation of the mechanisms of nanosilica particle-induced inflammation is necessary for the development of safe and effective nanosilica particles. Although nSP30 and nSP70 induced in vitro inflammatory responses, we did not detect the production of TNFα in vivo, perhaps owing to the timing of our measurement of TNFα production (Savici et al. 1994).

We also investigated the mechanisms of the inflammatory effects of nanosilica particles on RAW264.7 macrophages. Intracellular ROS function as second messengers of inflammatory effects by activating multiple signal pathways including a series of MAPKs (Thannickal and Fanburg 2000). The activation of MAPKs leads to the induction of transcription factors for TNFα production, such as nuclear factor κB, activator protein 1, and activating transcription factor (Bubici et al. 2006). These transcription factors control the inducible expression of genes of which the products are part of the inflammatory response. In fact, Ke et al. (2006) reported that ROS play an essential role in crystalline silica-induced TNFα production. Here, we demonstrated that smaller nanosilica particles activated MAPKs more strongly than did larger silica particles, and furthermore, we showed that nanosilica particle-induced intracellular ROS were important factors in nanosilica particle-induced inflammatory responses of macrophages (Figs. 2, 3). Consistent with our results, the recent results of Liu et al. showed that exposure to silica nanoparticles causes the generation of ROS in endothelial cells, which in turn induces endothelial apoptosis via JNK/p53 and evokes the activation of nuclear factor κB pathways (Liu and Sun 2010). These observations collectively suggest that nSP30- and nSP70-induced intracellular ROS may participate in the activation of MAPKs and subsequent inflammatory responses.

In contrast, our previous data showed that, by activating the cytoplasmic NOD-like receptor family member NLRP3 inflammasome, mSP1000 induce higher IL-1β production than do nanosilica particles (Morishige et al. 2010a). These results indicate that there are differences in the intracellular behavior, signaling pathways, and cytokine production profiles induced by silica particles of various sizes. Although the detailed mechanisms by which nano- and microsilica particles induce different signaling cascades remain unclear, recent reports have shown that nanomaterials are introduced into the macrophages via foreign-recognizing scavenger receptors rather than via the traditional endocytosis pathway (Iyer et al. 1996; Thakur et al. 2009). In particular, scavenger receptor class A-mediated recognition and ingestion of nanomaterials reportedly induce cytotoxicity and cytokine production via activation of p38 (Hirano et al. 2008; Limmon et al. 2008). Therefore, we speculate that the difference between the inflammatory effects of nano- and microsilica particles was due to differences in the pathways by which they are recognized and ingested.

We also examined the effect of surface modification on the inflammatory effects of silica particles, because particle surface properties have been demonstrated to be important factors for the particles' biological effects (Albrecht et al. 2004; He et al. 2008; Morishige et al. 2010a; Yamashita et al. 2011). Interestingly, although unmodified nSP70 and surface-modified nSP70-C were equally taken up, we found that nSP70-C did not induce inflammatory responses in vitro or in vivo (Figs. 4, 5a). Furthermore, nSP70-C induced less MAPK activation (Fig. 5b). These results indicate that changes in surface properties, such as the surface charge, suppressed the inflammatory responses induced by nSP70. We previously demonstrated that surface modification of mSP1000 with functional groups, including COOH groups, efficiently decreases mSP1000-induced ROS production (Morishige et al. 2010a). Therefore, we speculate that the nSP70-C triggered less ROS production (which induces TNFα production) than did unmodified nSP70, although more precise investigation is needed. It has recently been shown that nanomaterials become coated with serum proteins and induce different cellular responses by binding to proteins (Lesniak et al. 2010; Lundqvist et al. 2008). In addition, different surface characteristics, such as surface charge and surface functional groups, are known to influence the binding affinities of proteins to nanomaterials (Lundqvist et al. 2008). Therefore, the differences in protein binding between nSP70 and nSP70-C might have given rise to differences in the nanomaterials' inflammatory responses.

In addition to cytokine production, cell death induced by nanosilica particles is also a critical obstacle to the safety and efficacy of nanosilica particles, because macrophages play a central role in the defense system of the host. Our data indicate that nSP30 and nSP70 induced significant cell death and that their cytotoxicity might be dependent on p38 but independent of ERK and JNK signaling (Fig. 6). These results indicate that nanosilica particle-induced cell death depended on activation of p38, whereas nanosilica particle-induced production of TNFα was not involved in cell death. Consistent with these considerations, nSP70-C, which induces less MAPKs activation, did not trigger cell death.

We demonstrated that nanosilica particles induced stronger inflammatory responses than did microsilica particles and that nanosilica particle-induced TNFα production was mediated by the activation of ROS and MAPKs. Furthermore, by surface modification with COOH groups, we suppressed nanosilica particle-induced inflammatory responses by inhibiting the activation of MAPKs. We expect

that further studies of the relationship between surface characteristics and biological effects will provide useful information for the development of safe and effective nanomaterials.

Acknowledgments This work was supported by the Ministry of Health, Labor, and Welfare in Japan; the Ministry of Education, Culture, Sports, Science, and Technology of Japan; and the Global COE Program "in silico medicine" at Osaka University.

Conflict of interest The authors declare that they have no competing interests.

References

Albrecht C, Schins RP, Hohr D, Becker A, Shi T, Knaapen AM et al (2004) Inflammatory time course after quartz instillation: role of tumor necrosis factor-alpha and particle surface. Am J Respir Cell Mol Biol 31:292–301

Bharali DJ, Klejbor I, Stachowiak EK, Dutta P, Roy I, Kaur N et al (2005) Organically modified silica nanoparticles: a nonviral vector for in vivo gene delivery and expression in the brain. Proc Natl Acad Sci USA 102:11539–11544

Bottini M, D'Annibale F, Magrini A, Cerignoli F, Arimura Y, Dawson MI et al (2007) Quantum dot-doped silica nanoparticles as probes for targeting of T-lymphocytes. Int J Nanomedicine 2:227–233

Bubici C, Papa S, Dean K, Franzoso G (2006) Mutual cross-talk between reactive oxygen species and nuclear factor-kappa B: molecular basis and biological significance. Oncogene 25: 6731–6748

Busuttil SJ, Ploplis VA, Castellino FJ, Tang L, Eaton JW, Plow EF (2004) A central role for plasminogen in the inflammatory response to biomaterials. J Thromb Haemost 2:1798–1805

Chen Z, Meng H, Xing G, Yuan H, Zhao F, Liu R et al (2008) Age-related differences in pulmonary and cardiovascular responses to SiO2 nanoparticle inhalation: nanotoxicity has susceptible population. Environ Sci Technol 42:8985–8992

Decuzzi P, Godin B, Tanaka T, Lee SY, Chiappini C, Liu X et al (2010) Size and shape effects in the biodistribution of intravascularly injected particles. J Control Release 141:320–327

Dostert C, Petrilli V, Van Bruggen R, Steele C, Mossman BT, Tschopp J (2008) Innate immune activation through Nalp3 inflammasome sensing of asbestos and silica. Science 320: 674–677

He X, Nie H, Wang K, Tan W, Wu X, Zhang P (2008) In vivo study of biodistribution and urinary excretion of surface-modified silica nanoparticles. Anal Chem 80:9597–9603

Hirano S, Kanno S, Furuyama A (2008) Multi-walled carbon nanotubes injure the plasma membrane of macrophages. Toxicol Appl Pharmacol 232:244–251

Hirsch LR, Stafford RJ, Bankson JA, Sershen SR, Rivera B, Price RE et al (2003) Nanoshell-mediated near-infrared thermal therapy of tumors under magnetic resonance guidance. Proc Natl Acad Sci USA 100:13549–13554

Hornung V, Bauernfeind F, Halle A, Samstad EO, Kono H, Rock KL et al (2008) Silica crystals and aluminum salts activate the NALP3 inflammasome through phagosomal destabilization. Nat Immunol 9:847–856

Huaux F (2007) New developments in the understanding of immunology in silicosis. Curr Opin Allergy Clin Immunol 7:168–173

Iyer R, Hamilton RF, Li L, Holian A (1996) Silica-induced apoptosis mediated via scavenger receptor in human alveolar macrophages. Toxicol Appl Pharmacol 141:84–92

Jeffrey KL, Camps M, Rommel C, Mackay CR (2007) Targeting dual-specificity phosphatases: manipulating MAP kinase signalling and immune responses. Nat Rev Drug Discov 6:391–403

Kagan VE, Bayir H, Shvedova AA (2005) Nanomedicine and nanotoxicology: two sides of the same coin. Nanomedicine 1:313–316

Ke Q, Li J, Ding J, Ding M, Wang L, Liu B et al (2006) Essential role of ROS-mediated NFAT activation in TNF-alpha induction by crystalline silica exposure. Am J Physiol Lung Cell Mol Physiol 291:L257–L264

Kops SK, Ratzlaff RE, Meade R, Iverson GM, Askenase PW (1986) Interaction of antigen-specific T cell factors with unique "receptors" on the surface of mast cells: demonstration in vitro by an indirect rosetting technique. J Immunol 136:4515–4524

Lesniak A, Campbell A, Monopoli MP, Lynch I, Salvati A, Dawson KA (2010) Serum heat inactivation affects protein corona composition and nanoparticle uptake. Biomaterials 31:9511–9518

Li X, Hu Y, Jin Z, Jiang H, Wen J (2009) Silica-induced TNF-alpha and TGF-beta1 expression in RAW264.7 cells are dependent on Src-ERK/AP-1 pathways. Toxicol Mech Methods 19:51–58

Limmon GV, Arredouani M, McCann KL, Corn Minor RA, Kobzik L, Imani F (2008) Scavenger receptor class-A is a novel cell surface receptor for double-stranded RNA. Faseb J 22:159–167

Liu X, Sun J (2010) Endothelial cells dysfunction induced by silica nanoparticles through oxidative stress via JNK/P53 and NF-kappaB pathways. Biomaterials 31:8198–8209

Lundqvist M, Stigler J, Elia G, Lynch I, Cedervall T, Dawson KA (2008) Nanoparticle size and surface properties determine the protein corona with possible implications for biological impacts. Proc Natl Acad Sci USA 105:14265–14270

Mantovani A, Allavena P, Sica A, Balkwill F (2008) Cancer-related inflammation. Nature 454:436–444

Mitchell LA, Lauer FT, Burchiel SW, McDonald JD (2009) Mechanisms for how inhaled multiwalled carbon nanotubes suppress systemic immune function in mice. Nat Nanotechnol 4:451–456

Morel F, Doussiere J, Vignais PV (1991) The superoxide-generating oxidase of phagocytic cells. Physiological, molecular and pathological aspects. Eur J Biochem 201:523–546

Morishige T, Yoshioka Y, Inakura H, Tanabe A, Yao X, Narimatsu S et al (2010a) The effect of surface modification of amorphous silica particles on NLRP3 inflammasome mediated IL-1beta production, ROS production and endosomal rupture. Biomaterials 31:6833–6842

Morishige T, Yoshioka Y, Tanabe A, Yao X, Tsunoda S, Tsutsumi Y et al (2010b) Titanium dioxide induces different levels of IL-1beta production dependent on its particle characteristics through caspase-1 activation mediated by reactive oxygen species and cathepsin B. Biochem Biophys Res Commun 392:160–165

Mossman BT, Churg A (1998) Mechanisms in the pathogenesis of asbestosis and silicosis. Am J Respir Crit Care Med 157: 1666–1680

Nel A, Xia T, Madler L, Li N (2006) Toxic potential of materials at the nanolevel. Science 311:622–627

Poland CA, Duffin R, Kinloch I, Maynard A, Wallace WA, Seaton A et al (2008) Carbon nanotubes introduced into the abdominal cavity of mice show asbestos-like pathogenicity in a pilot study. Nat Nanotechnol 3:423–428

Roy I, Ohulchanskyy TY, Bharali DJ, Pudavar HE, Mistretta RA, Kaur N et al (2005) Optical tracking of organically modified silica nanoparticles as DNA carriers: a nonviral, nanomedicine approach for gene delivery. Proc Natl Acad Sci USA 102:279–284

Sager TM, Kommineni C, Castranova V (2008) Pulmonary response to intratracheal instillation of ultrafine versus fine titanium dioxide: role of particle surface area. Part Fibre Toxicol 5:17

Savici D, He B, Geist LJ, Monick MM, Hunninghake GW (1994) Silica increases tumor necrosis factor (TNF) production, in part, by upregulating the TNF promoter. Exp Lung Res 20:613–625

Shiryaev A, Moens U (2010) Mitogen-activated protein kinase p38 and MK2, MK3 and MK5: menage a trois or menage a quatre? Cell Signal 22:1185–1192

Takagi A, Hirose A, Nishimura T, Fukumori N, Ogata A, Ohashi N et al (2008) Induction of mesothelioma in p53± mouse by intraperitoneal application of multi-wall carbon nanotube. J Toxicol Sci 33:105–116

Thakur SA, Hamilton R Jr, Pikkarainen T, Holian A (2009) Differential binding of inorganic particles to MARCO. Toxicol Sci 107:238–246

Thannickal VJ, Fanburg BL (2000) Reactive oxygen species in cell signaling. Am J Physiol Lung Cell Mol Physiol 279:L1005–L1028

Verraedt E, Pendela M, Adams E, Hoogmartens J, Martens JA (2009) Controlled release of chlorhexidine from amorphous microporous silica. J Control Release 142:47–52

Waters KM, Masiello LM, Zangar RC, Tarasevich BJ, Karin NJ, Quesenberry RD et al (2009) Macrophage responses to silica nanoparticles are highly conserved across particle sizes. Toxicol Sci 107:553–569

Yamashita K, Yoshioka Y, Higashisaka K, Morishita Y, Yoshida T, Fujimura M et al (2010) Carbon nanotubes elicit DNA damage and inflammatory response relative to their size and shape. Inflammation 33:276–280

Yamashita K, Yoshioka Y, Higashisaka K, Mimura K, Morishita Y, Nozaki M et al (2011) Silica and titanium dioxide nanoparticles cause pregnancy complications in mice. Nat Nanotechnol 6:321–328

Yang X, Liu J, He H, Zhou L, Gong C, Wang X et al (2010) SiO2 nanoparticles induce cytotoxicity and protein expression alteration in HaCaT cells. Part Fibre Toxicol 7:1

—Foreword—

ナノマテリアルの安全確保に向けたNanoTox研究の最前線

堤　康央,*,a,b 吉岡靖雄b

Recent Topics of NanoTox Studies for Their Safety

Yasuo TSUTSUMI*,a,b and Yasuo YOSHIOKAb

aDepartment of Toxicology and Safety Science, Graduate School of Pharmaceutical Sciences, and bThe Center for Advanced Medical Engineering and Informatics, Osaka University, 1–6 Yamadaoka, Suita, Osaka 565–0871, Japan

2000年1月に，当時の米国クリントン大統領が「国家ナノテクノロジー戦略」を発表し，大規模国家予算を投資したことが1つの起爆剤となり，ナノマテリアルの開発研究と生産，そして実用化が，国内外の産官学を問わず，多くの領域（医療，情報，環境，エネルギーなど）で急速に進展した．ナノマテリアルとは，少なくとも一次元の大きさが100 nm以下で製造された超微細材料と定義されている（毛髪の太さ：50 μmの500分の1以下）．このナノマテリアルは，従来までのサブミクロンサイズ以上（100 nm以上）の素材とは異なり，サイズ減少に伴う組織浸透性の増大や電子反応性の増大，重量あたりの表面積の増加などにより，抗酸化効果や紫外線遮蔽効果といった有用機能が格段に向上しており，われわれの生活の質的向上に革命を起こすものと期待されている．わが国においても，2001年の第二期科学技術基本計画において，ナノテクノロジーが重点4分野に指定されて以降，ナノマテリアルの開発・実用化の点で世界をリードしている．例えば，医薬品・食品・化粧品領域では，ナノシリカやナノ酸化チタン，フラーレン，白金ナノコロイド，ナノシルバーなどが既に，必須素材として上市されており，薬学領域においても次世代を担う新素材として期待されている．

一方で，ナノマテリアルの物性（サイズ，形状など）に起因した革新的機能が逆に，二面性を呈してしまい，サブミクロンサイズ以上の従来型素材では観察されない，特徴的な毒性，いわゆる，ナノトックス（NanoTox）を発現してしまうことが世界的に懸念されている．例えば，今後の詳細な検証が必要ではあるものの，ある種のカーボンナノチューブが，アスベストと同様に吸引曝露により悪性中皮腫を誘発し得ることが報告されている．そのため，経済協力開発機構（OECD）と連携しつつ，欧米各国などはナノマテリアルの開発やその利用を規制しようとする動きを加速している．わが国でも厚労省や経産省，環境省，内閣府を中心にナノマテリアルの安全性評価研究が今，まさにスタートしたところであるが，知財技術立国を目指すわが国としては，ナノマテリアルの開発・実用化を闇雲に規制するのではなく，ナノテクノロジーの恩恵を社会が最大限に享受できるよう，ナノ産業の育成や発展を強力に支援しつつ，一方で責任ある先進国，そして健康立国として，ナノマテリアルの安全性を高度に保障し，ヒトの健康環境を確保していかねばならない．すなわち，私心ではあるが，今後，わが国としては，ナノマテリアルの毒性研究（NanoTox研究）ではなく，いかに安全で安心，かつ有用なナノマテリアルの開発と実用化支援の観点から，ナノマテリアルの安全科学研究（Nano Safety Science）の推進こそが重要となってこよう．

本観点から，本シンポジウムでは，医薬品や化粧品，食品等に利用・実用化されているナノマテリアルに焦点を絞り，その安全性研究の最前線を紹介して頂き，薬学的観点から将来展望等を議論して頂いた．今後，わが国としては，これらナノマテリアルの安全性評価，あるいは安全性確保研究を積み重ね

aDepartment of Toxicology and Safety Science, Graduate School of Pharmaceutical Sciences, and bThe Center for Advanced Medical Engineering and Informatics, Osaka University, 1–6 Yamadaoka, Suita, Osaka 565–0871, Japan
*e-mail: ytsutsumi@phs.osaka-u.ac.jp

日本薬学会第130年会シンポジウムS18序文

ることで，安全なナノマテリアルの開発と実用化を促進し，一方でヒトの健康環境を確保し得るものと期待しており，本シンポジウムがその一助となったものと確信している．

Genes and Environment, Vol. 33, No. 1 pp. 21–26 (2011)

Review

Safety Evaluation Study of Nanomaterials Aimed at Promoting Their Acceptance by Society

Hiromi Nabeshi[1,2,4], Tomoaki Yoshikawa[1,2], Yasuo Yoshioka[2,3] and Yasuo Tsutsumi[1,2,3,4]

[1]Department of Toxicology and Safety Science, Graduate School of Pharmaceutical Sciences, Osaka University, Osaka, Japan
[2]Laboratory of Biopharamceutical Research, National Institute of Biomedical Innovation, Osaka, Japan
[3]The Center for Advanced Medical Engineering and Informatics, Osaka University, Osaka, Japan

(Received November 13, 2010; Revised December 20, 2010; Accepted December 27, 2010)

Currently, nanomaterials (NMs) with particle sizes below 100 nm have been successfully employed in various industrial applications in medicine, cosmetics and foods. On the other hand, NMs can also be problematic in terms of eliciting harmful effects as a result of their small size. However, biological and/or cellular responses to NMs are often inconsistent and even contradictory. In addition, relationships among the physicochemical properties, localization and biological responses of NMs are not yet well understood. In order to open new frontiers in the use of the safer NMs in the fields of medicine, cosmetics and foods, it is necessary to understand the detailed properties of NMs so that their safety can be predicted. In this review, we present some of our studies examining the cellular localization and cytotoxicity, including genotoxic effects of well-dispersed amorphous silica particles of diameters ranging from 70 nm to 1000 nm. Our results suggest that "well-dispersed" amorphous nanosilica of particle size 70 nm (nSP70) enters the nucleus and exhibits mutagenic activity related in ROS generation *in vitro*. Our data indicate that further studies of the relation between the physicochemical properties of, and the biological responses to NMs are needed to ensure the safety of these materials, and to promote their acceptance by society.

Key words: nanosilicas, genotoxicity, reactive oxygen species generation

Introduction

In January 2000, US President Bill Clinton advocated for the National Nanotechnology Initiative (NNI) and began a massive investment in nanotechnology research and development. This US policy resulted in an explosion of research on the development of nanotechnology-based applications in wide-ranging fields, including information technology, energy and medicine. The recent development of nanoscale engineering represents a dynamic area of interdisciplinary research, incorporating nanomaterials (NMs) into a diverse product matrix, including diagnostics, food additives and cosmetics. Because amorphous silica nanoparticles (nSPs) and titanium oxide nanoparticles are colorless and reflect ultraviolet radiation more efficiently than micro-sized particles, nSPs and titanium oxide nanoparticles are already used as cosmetic vehicles or functional ingredients in many cosmetics such as foundation creams and sunscreens (1,2). An NM is defined as a substance that has at least one dimension of less than 100 nm in size. NMs can assume many different forms, such as tubes, rods, wires, spheres or particles. Because they exhibit unique physicochemical properties and innovative functions, the world market for NMs is expected to significantly increase during the next few years (3).

However, because NMs may possess novel properties, kinetics, and biological effects different from those of micro size bulk materials, their potential for harmful effects on humans is raising concerns about their safety. For example, exposure of cells or animals to carbon nanotubes, TiO_2 nanoparticles or silver nanoparticles have been reported to induce cytotoxicity and inflammation (4–16). However, other researchers have reported that carbon nanotubes and TiO_2 nanoparticles do not induce harmful effects (17–19). Thus, despite intensive research efforts, investigations of biological and/or cellular responses to NMs are often inconsistent and even contradictory. In addition, relationships among the physicochemical properties, absorbency, and localization of, and biological responses to NMs are not yet well understood. In order to ensure the safety of NMs and open new frontiers for the use of NMs in biological fields, it is necessary to gain a more complete understanding of NMs. For example, in order to build a comprehensive prediction system of the safety of NMs, it

[4]Correspondence to: Hiromi Nabeshi and Yasuo Tsutsumi, Department of Toxicology and Safety Science, Graduate School of Pharmaceutical Sciences, Osaka University, 1-6, Yamadaoka, Suita, Osaka 565-0871, Japan. Tel: +81-6-6879-8233, Fax: +81-6-6879-8233, E-mail: nabeshi@phs.osaka-u.ac.jp and ytsutsumi@phs.osaka-u.ac.jp

would be helpful to explore the detailed properties of NMs and the relationship among their physicochemical properties, absorbency, and localization, and the biological responses they elicit from the point of view of biosafety (Our strategy is summarized in Fig. 1).

Physicochemical Properties of Various-sized Silica Particles

In this study, we used amorphous nanosilica particles (nSPs) as an example of an NM. nSPs are one of the most widely applied NMs, and are used in cosmetics and food additives. nSPs also have great potential for use as diagnostic imaging agents, gene delivery carriers and cancer therapies (20–24). In addition, these NMs show overwhelmingly superior dispersibility as compared with carbon nanotubes, fullerene and nano-sized TiO_2. Thus, these nSPs are ideally suited for determining how particle size influences cellular responses to NMs.

We first analyzed the physicochemical properties of commercially available silica particles of 70, 300 and 1000 nm in diameter (nSP70, nSP300 and mSP1000, respectively). Close examination of the silica particles of different particle sizes by transmission electron microscopy (TEM) and scanning electron microscopy (SEM) revealed that all silica particles used in this study were smooth-surfaced spherical particles, and that the primary particle sizes were approximately uniform (Fig. 2). The mean size and the mean zeta potential of silica particles in a neutral solvent for each size category are also shown in Fig. 2. These results suggest that the silica particles used in this study remained as stable well-dispersed particles in solution, and did not form aggregates. Thus, these particles are ideally suited to evaluate whether their bio-distribution and biological effects depend on particle size.

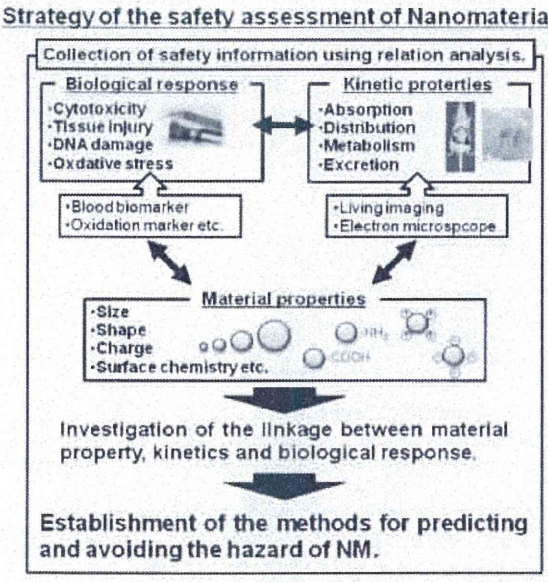

Fig. 1. Our strategy for the safety assessment of nanomaterials.

Analysis of Intracellular Distribution of Silica Particles in Human Keratinocytes

It has been reported that NMs can enter the skin by transdermal exposure (25–27). These reports indicate the possibility that NMs enter and accumulate in the human body after dermal exposure over a relative long time period. Accordingly, in this study, we evaluated the intracellular distribution of, and cellular responses to silica particles in skin cells.

	Nanosilica	Conventional silica (over 100 nm)	
	nSP70	nSP300	mSP1000
Size (nm)	70	300	1000
SEM images	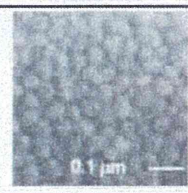	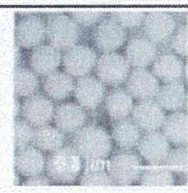	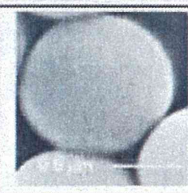
Particle size in solution (nm)	69.4 ± 7.7	356 ± 14.6	1390 ± 92
Surface charge (mV)	-57.1 ± 8.1	-63.0 ± 1.6	-82.1 ± 2.1

Fig. 2. Scanning electron microscopy (SEM) analysis, particle size and zeta potential of silica particles. SEM photomicrographs of silica particles used in this study: nSP70, nSP300 and mSP1000. Scale bars: 0.1 μm (nSP70) and 0.5 μm (nSP300 and mSP1000). Results are expressed as mean ± S.D. ($n=3$).

Firstly, to determine the intracellular location of silica particles, we used TEM to examine HaCaT cells that were treated with 100 μg/ml of nSP70, nSP300, or mSP1000. TEM examination revealed the presence of mSP1000 and nSP300 particles only in the endosome. Cells treated with mSP1000 were also found to contain a large number of lysosomes. In contrast, in nSP70-treated cells nSP70 particles were present in the cytoplasm as well as in the nucleus. Furthermore, nSP70 particles accumulated in the nucleolus. Recently, it has been reported that the intracellular localization of NMs may be linked to the induction of harmful effects. For example, the localization of silver nanoparticles in the nucleus and mitochondria may be related to mitochondrial dysfunction or oxidative stress (28). Thus, analysis of intracellular localization may provide important and useful information to predict nanotoxicity.

Analysis of Cell-growth Inhibition and Genotoxicity Induced by Silica Particles

Next, we investigated the biological effects of nSPs. To this end, we assessed the effects of nSPs of various particle sizes on the proliferation of HaCaT cells. We found that cell proliferation was inhibited following treatment with nSP70 and nSP300 in a both dose- and size-dependent manner. The half maximal (50%) inhibitory concentration (IC_{50}) of nSP70 and nSP300 for cell proliferation was 323 and 3966 μg/ml, respectively. We were, however, unable to calculate the IC_{50} of mSP1000. Taken together, these results suggested that smaller sized silica particles inhibited the growth of HaCaT cells more strongly than the larger particles.

Based on evidence of nuclear entry of nSP70 *in vivo* and *in vitro*, we next evaluated the effects of nSPs on DNA damage. We used the comet assay to analyze DNA single strand breaks in nSP-treated HaCaT cells. As shown in Table 1, in cells treated with PBS (negative control) for 3 h, the average tail length was 23.3 μm. In cells treated with 90 μg/ml of nSP70, nSP300, or mSP1000, the average tail lengths were 102.9 μm, 30.5 μm, and 22.5 μm, respectively. The average tail lengths increased with decreasing size of the silica particles. The tail lengths found in the nSP70-treated cells were longer than those found in the positive control cells (0.2 mM H_2O_2 treated cells) (Table 1). These findings suggest the possibility that nSPs with particle sizes below 100 nm could induce mutations.

Table 1. Detection of DNA strand breaks induced by treatment with silica particles using the comet assay

	Tail length (μm)		
Concentration		30 μg/ml	90 μg/ml
PBS	23.3±8.6	—	—
0.2 mM H_2O_2	64.5±2.8	—	—
nSP70		99.9±23.2*	102.9±15.2*
nSP300		26.3±4.6	30.5±8.9
mSP1000		30.7±9.5	22.5±3.2

HaCaT cells were treated with test materials for 3 h. Data shown are mean±SD of at least 16 cells for each sample. *Significant increase ($P<0.01$) compared with the negative control, PBS.

Analysis of the Mechanism of Cell-growth Inhibition and Genotoxicity Induced by Silica Particles Focusing on Reactive Oxygen Species

Many reports have indicated that intracellular generation of reactive oxygen species (ROS) is induced by various types of nanoparticles, such as carbon black, nano-sized TiO_2 and nano-sized silver particles (28–41). Furthermore, it has recently been reported that crystalline silica induces intracellular ROS generation via NADPH oxidase activation following uptake by endocytosis (42,43). Based on these reports, ROS generation and DNA damage are obvious indicators for assessing the hazards posed by nSPs. Firstly, total intracellular ROS generation was measured in silica particle-treated HaCaT cells using 2′7′-dichlorodihydorofluorescein diacetate (DCFH-DA) (Fig. 3). Silica particles of all sizes were found to induce intracellular ROS generation in a dose-dependent fashion. However, ROS generation by nSP70 treatment was significantly greater compared with that generated by nSP300 and mSP1000 treatment at the same particle concentration. These results suggested that silica particle-induced intracellular ROS generation was significantly increased by decreasing the particle size to less than 100 nm. It is well-known that

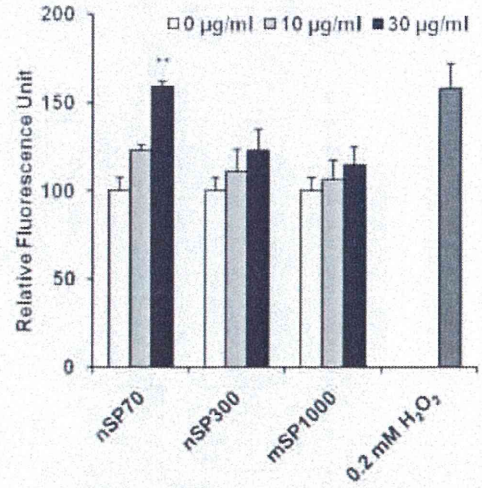

Fig. 3. Detection of oxidative stress induced by silica particle treatment in HaCaT cells. Detection of total ROS and hydroxyl radicals induced by silica particle treatment in HaCaT cells. HaCaT cells were incubated with various concentrations of nSP70, nSP300, and mSP1000 for 3 h. 0.2 mM H_2O_2 were used as positive control. **$P<0.01$ vs PBS.

intracelluler ROS induces oxidative DNA damage related to mutagenesis, carcinogenesis and the aging process (44–47). These results suggest the possibility that nSP70 may be genotoxic.

A number of mechanisms underlie the ability of nanoparticles to cause DNA damage. As mentioned above, a key mechanism that is often described is the ability of particles to cause the production of ROS (1,48). One possible mechanism of particle-mediated DNA damage is the ability of particles to stimulate target cells to produce oxidants/genotoxic compounds, e.g., by affecting mitochondrial electron transport, activation of NADPH oxidase, or inducing cytochrome P450 enzymes. Alternatively, the physical and chemical properties of the particles themselves may be sufficient to generate oxidants, thereby leading to DNA damage. In addition to the mechanism of DNA damage involving the generation of ROS, nanoparticles may gain direct access to DNA via nuclear transport. This seems very unlikely, however, given that the nuclear pore complex is less than 8 nm in diameter (49). Nonetheless, some studies have reported that nanoparticles such as silica nanoparticles (40–70 nm) (50) or silver nanoparticles (6–20 nm) can penetrate the nuclear membrane (28). A detailed analysis of the mechanism of DNA damage induced by nanoparticles is currently underway. This information will be a critical determinant in the design of safer nSPs and will provide valuable information for hazard assessment of nSPs.

Conclusions

In this review, we report that compared with bulk material of particle sizes above the nanoscale (above 100 nm), "well-dispersed" amorphous nanosilica with a particle size of 70 nm shows different bio-properties with respect to entry into the nucleus. These bio-properties show the potential for nanosilica to act as a new functional material, but as a result of these differences, nSP70 exerts various adverse cellular responses in skin cells, such as ROS generation and DNA damage. By contrast, bulk-sized materials of larger particle size display a much reduced response. These different responses might be partly due to different mechanisms, such as intracellular uptake and ROS generation. We speculated that receptor-mediated uptake was involved in these phenomena, and set out to identify the physicochemical properties that affect receptor endocytosis. We expect that more information provided by further studies of the relationship between the physicochemical properties of, and biological responses to NMs will lead to an acceptance by society of the safety and usefulness of these materials. In addition, we believe a detailed analysis of nSP-internalization will be invaluable for both hazard assessment and the design of safe nSPs.

Acknowledgement: This study was supported in part by Grants-in-Aid for Scientific Research from the Ministry of Education, Culture, Sports, Science and Technology of Japan, and from the Japan Society for the Promotion of Science (JSPS). This study was also supported in part by Health Labour Sciences Research Grants from the Ministry of Health, Labor and Welfare of Japan; by Health Sciences Research Grants for Research on Publicly Essential Drugs and Medical Devices from the Japan Health Sciences Foundation; by a Global Environment Research Fund from the Minister of the Environment; and by a the Knowledge Cluster Initiative; the Food Safety Commission; The Nagai Foundation Tokyo; The Cosmetology Research Foundation; The Smoking Research Foundation; and The Takeda Science Foundation.

References

1 Nel A, Xia T, Madler L, Li N. Toxic potential of materials at the nanolevel. Science. 2006; 311: 622–7.
2 SCENIHR. EU. Scientific Comittee on Emerging and Newly Identified Health Risks. Opinion on thé appropriateness of existing méthodologies to assess thé potential risks associated with engineered and adventitious products of nanotechnologies. European Commission, Health and Consumer Protection, Directorate Général, 28–29 September, 2005.
3 The Royal Society & The Royal Academy of Engineering. Nanoscience and nanotechnologies. 2004; Chapter 4: p. 25–34. http://www.nanotec.org.uk/report/chapter4.pdf
4 Aiso S, Yamazaki K, Umeda Y, Asakura M, Takaya M, Toya T, Koda S, Nagano K, Arito H, Fukushima S. Pulmonary toxicity of intratracheally instilled multiwall carbon nanotubes in male Fischer 344 rats. Ind Health. 2010; 48: 783–95.
5 Chen J, Dong X, Zhao J, Tang G. *In vivo* acute toxicity of titanium dioxide nanoparticles to mice after intraperitioneal injection. J Appl Toxicol. 2009; 29: 330–7.
6 Geys J, Nemmar A, Verbeken E, Smolders E, Ratoi M, Hoylaerts MF, Nemery B, Hoet PH. Acute toxicity and prothrombotic effects of quantum dots: impact of surface charge. Environ Health Perspect. 2008;116: 1607–13.
7 Heng BC, Zhao X, Xiong S, Ng KW, Boey FY, Loo JS. Toxicity of zinc oxide (ZnO) nanoparticles on human bronchial epithelial cells (BEAS-2B) is accentuated by oxidative stress. Food Chem Toxicol. 2010; 48: 1762–6.
8 Kocbek P, Teskac K, Kreft ME, Kristl J. Toxicological aspects of long-term treatment of keratinocytes with ZnO and TiO_2 nanoparticles. Small. 2010; 6: 1908–17.
9 Liu S, Xu L, Zhang T, Ren G, Yang Z. Oxidative stress and apoptosis induced by nanosized titanium dioxide in PC12 cells. Toxicology. 2010; 267: 172–7.
10 Moos PJ, Chung K, Woessner D, Honeggar M, Cutler NS, Veranth JM. ZnO particulate matter requires cell contact for toxicity in human colon cancer cells. Chem Res Toxicol. 2010; 23: 733–9.
11 Murray AR, Kisin E, Leonard SS, Young SH, Kommineni C, Kagan VE, Castranova V, Shvedova AA. Oxidative

stress and inflammatory response in dermal toxicity of single-walled carbon nanotubes. Toxicology. 2009; 257: 161–71.

12 Park EJ, Kim H, Kim Y, Yi J, Choi K, Park K. Carbon fullerenes (C60s) can induce inflammatory responses in the lung of mice. Toxicol Appl Pharmacol. 2010; 244: 226–33.

13 Poland CA, Duffin R, Kinloch I, Maynard A, Wallace WA, Seaton A, Stone V, Brown S, Macnee W, Donaldson K. Carbon nanotubes introduced into the abdominal cavity of mice show asbestos-like pathogenicity in a pilot study. Nat Nanotechnol. 2008; 3: 423–8.

14 Shin JA, Lee EJ, Seo SM, Kim HS, Kang JL, Park EM. Nanosized titanium dioxide enhanced inflammatory responses in the septic brain of mouse. Neuroscience. 2010; 165: 445–54.

15 Takagi A, Hirose A, Nishimura T, Fukumori N, Ogata A, Ohashi N, Kitajima S, Kanno J. Induction of mesothelioma in $p53^{+/-}$ mouse by intraperitoneal application of multi-wall carbon nanotube. J Toxicol Sci. 2008; 33: 105–16.

16 Yamashita K, Yoshioka Y, Higashisaka K, Morishita Y, Yoshida T, Fujimura M, Kayamuro H, Nabeshi H, Yamashita T, Nagano K, Abe Y, Kamada H, Kawai Y, Mayumi T, Yohikawa T, Itoh N, Tsunoda S, Tsutsumi Y. Carbon nanotubes elicit DNA damage and inflammatory response relative to their size and shape. Inflammation. 2010; 33: 276–80.

17 Chlopek J, Czajkowaska B, Szaraniec B, Frackowiak E, Szostak K, Beguin F. *In vitro* studies of carbon nanotubes biocompatibility. Carbon. 2006; 44: 1106–11.

18 Singh S, Shi T, Duffin R, Albrecht C, van Berlo D, Hohr D, Fubini B, Martra G, Fenoglio I, Borm PJ, Schins RP. Endocytosis, oxidative stress and IL-8 expression in human lung epithelial cells upon treatment with fine and ultrafine TiO_2: role of the specific surface area and of surface methylation of the particles. Toxicol Appl Pharmacol. 2007; 222: 141–51.

19 Thibodeau M, Giardina C, Hubbard AK. Silica-induced caspase activation in mouse alveolar macrophages is dependent upon mitochondrial integrity and aspartic proteolysis. Toxicol Sci. 2003; 76: 91–101.

20 Bharali DJ, Klejbor I, Stachowiak EK, Dutta P, Roy I, Kaur N, Bergey EJ, Prasad PN, Stachowiak MK. Organically modified silica nanoparticles: a nonviral vector for *in vivo* gene delivery and expression in the brain. Proc Natl Acad Sci USA. 2005; 102: 11539–44.

21 Bottini M, D'Annibale F, Magrini A, Cerignoli F, Arimura Y, Dawson MI, Bergamaschi E, Rosato N, Bergamasch A, Mustelin T. Quantum dot-doped silica nanoparticles as probes for targeting of T-lymphocytes. Int J Nanomedicine. 2007; 2: 227–33.

22 Hirsch LR, Stafford RJ, Bankson JA, Sershen SR, Rivera B, Price RE, Hazle JD, Halas NJ, West JL. Nanoshell-mediated near-infrared thermal therapy of tumors under magnetic resonance guidance. Proc Natl Acad Sci U S A. 2003; 100: 13549–54.

23 Roy I, Ohulchanskyy TY, Bharali DJ, Pudavar HE, Mistretta RA, Kaur N, Prasad PN. Optical tracking of organically modified silica nanoparticles as DNA carriers: a nonviral, nanomedicine approach for gene delivery. Proc Natl Acad Sci USA. 2005; 102: 279–84.

24 Verraedt E, Pendela M, Adams E, Hoogmartens J, Martens JA. Controlled release of chlorhexidine from amorphous microporous silica. J Control Release. 2010; 142: 47–52.

25 Larese FF, D'Agostin F, Crosera M, Adami G, Renzi N, Bovenzi M, Maina G. Human skin penetration of silver nanoparticles through intact and damaged skin. Toxicology. 2009; 255: 33–7.

26 Mortensen LJ, Oberdorster G, Pentland AP, Delouise LA. *In vivo* skin penetration of quantum dot nanoparticles in the murine model: the effect of UVR. Nano Lett. 2008; 8: 2779–87.

27 Wu J, Liu W, Xue C, Zhou S, Lan F, Bi L, Xu H, Yang X, Zeng FD. Toxicity and penetration of TiO_2 nanoparticles in hairless mice and porcine skin after subchronic dermal exposure. Toxicol Lett. 2009; 191: 1–8.

28 AshaRani PV, Low Kah Mun G, Hande MP, Valiyaveettil S. Cytotoxicity and genotoxicity of silver nanoparticles in human cells. ACS Nano 2009; 3: 279–90.

29 Eom HJ, Choi J. Oxidative stress of silica nanoparticles in human bronchial epithelial cell, Beas-2B. Toxicol *In Vitro*. 2009; 23: 1326–32.

30 Fahmy B, Cormier SA. Copper oxide nanoparticles induce oxidative stress and cytotoxicity in airway epithelial cells. Toxicol *In Vitro*. 2009; 23: 1365–71.

31 Foldbjerg R, Olesen P, Hougaard M, Dang DA, Hoffmann HJ, Autrup H. PVP-coated silver nanoparticles and silver ions induce reactive oxygen species, apoptosis and necrosis in THP-1 monocytes. Toxicol Lett. 2009; 190: 156–62.

32 Hussain S, Boland S, Baeza-Squiban A, Hamel R, Thomassen LC, Martens JA, Billon-Galland MA, Fleury-Feith J, Moisan F, Pairon JC, Marano F. Oxidative stress and proinflammatory effects of carbon black and titanium dioxide nanoparticles: role of particle surface area and internalized amount. Toxicology. 2009; 260: 142–9.

33 Karlsson HL, Gustafsson J, Cronholm P, Moller L. Size-dependent toxicity of metal oxide particles—a comparison between nano- and micrometer size. Toxicol Lett. 2009; 188: 112–8.

34 Kim S, Choi JE, Choi J, Chung KH, Park K, Yi J, Ryu DY. Oxidative stress-dependent toxicity of silver nanoparticles in human hepatoma cells. Toxicol *In Vitro*. 2009; 23: 1076–84.

35 Li KG, Chen JT, Bai SS, Wen X, Song SY, Yu Q, Li J, Wang YQ. Intracellular oxidative stress and cadmium ions release induce cytotoxicity of unmodified cadmium sulfide quantum dots. Toxicol *In Vitro*. 2009; 23: 1007–13.

36 Liu S, Xu L, Zhang T, Ren G, Yang Z. Oxidative stress and apoptosis induced by nanosized titanium dioxide in PC12 cells. Toxicology. 2010; 267: 172–7.

37 Pan Y, Leifert A, Ruau D, Neuss S, Bornemann J, Schmid G, Brandau W, Simon U, Jahnen-Dechent W. Gold nanoparticles of diameter 1.4 nm trigger necrosis by oxidative stress and mitochondrial damage. Small. 2009;

5: 2067–76.

38 Park EJ, Park K. Oxidative stress and pro-inflammatory responses induced by silica nanoparticles *in vivo* and *in vitro*. Toxicol Lett. 2009; 184: 18–25.

39 Wang F, Gao F, Lan M, Yuan H, Huang Y, Liu J. Oxidative stress contributes to silica nanoparticle-induced cytotoxicity in human embryonic kidney cells. Toxicol *In Vitro*. 2009; 23: 808–15.

40 Xia T, Kovochich M, Brant J, Hotze M, Sempf J, Oberley T, Sioutas C, Yeh JI, Wiesner MR, Nel AE. Comparison of the abilities of ambient and manufactured nanoparticles to induce cellular toxicity according to an oxidative stress paradigm. Nano Lett. 2006; 6: 1794–807.

41 Yamakoshi Y, Umezawa N, Ryu A, Arakane K, Miyata N, Goda Y, Masumizu T, Nagano T. Active oxygen species generated from photoexcited fullerene (C60) as potential medicines: O2-* versus $^1O_2$. J Am Chem Soc. 2003; 125: 12803–9.

42 Dostert C, Petrilli V, Van Bruggen R, Steele C, Mossman BT, Tschopp J. Innate immune activation through Nalp3 inflammasome sensing of asbestos and silica. Science 2008; 320: 674–7.

43 Hornung V, Bauernfeind F, Halle A, Samstad EO, Kono H, Rock KL, Fitzgerald KA, Latz E. Silica crystals and aluminum salts activate the NALP3 inflammasome through phagosomal destabilization. Nat Immunol. 2008; 9: 847–56.

44 Ames BN. Dietary carcinogens and anticarcinogens. Oxygen radicals and degenerative diseases. Science. 1983; 221: 1256–64.

45 Harman D. The aging process. Proc Natl Acad Sci USA. 1981; 78: 7124–8.

46 Takeuchi T, Morimoto K. Crocidolite asbestos increased 8-hydroxydeoxyguanosine levels in cellular DNA of a human promyelocytic leukemia cell line, HL60. Carcinogenesis 1994; 15: 635–9.

47 Takeuchi T, Nakajima M, Morimoto K. Establishment of a human system that generates O2- and induces 8-hydroxydeoxyguanosine, typical of oxidative DNA damage, by a tumor promotor. Cancer Res. 1994; 54: 5837–40.

48 Schins RP. Mechanisms of genotoxicity of particles and fibers. Inhal Toxicol. 2002; 14: 57–78.

49 Terry LJ, Shows EB, Wente SR. Crossing the nuclear envelope: hierarchical regulation of nucleocytoplasmic transport. Science. 2007; 318: 1412–6.

50 Chen M, von Mikecz A. Formation of nucleoplasmic protein aggregates impairs nuclear function in response to SiO_2 nanoparticles. Exp Cell Res. 2005; 305: 51–62.

食品分野におけるナノテクノロジーの安全性

Safety of Nanotechnology in the Field of Foods

[1] 大阪大学薬学研究科毒性学分野
[2] 独立行政法人医薬基盤研究所バイオ創薬プロジェクト
[3] 大阪大学臨床医工学融合研究教育センター

鍋師裕美[1,2]，吉岡靖雄[1,2,3]，吉川友章[1,2]，堤　康央[1,2,3]

[1] Department of Toxicology and Safety Science, Graduate School of Pharmaceutical Sciences, Osaka University
[2] Laboratory of Biopharmaceutical Research (LBR), National Institute of Biomedical Innovation (NiBio)
[3] The Center for Advanced Medical Engineering and Informatics

Hiromi NABESHI[1,2], Yasuo YOSHIOKA[1,2,3], Tomoaki YOSHIKAWA[1,2], Yasuo TSUTSUMI[1,2,3]

I　はじめに

近年，ナノテクノロジーが劇的に進展したことによって，ナノマテリアルの開発研究と生産，そして実用化が，国内外の産官学を問わず，多くの領域で急速に進展している。ナノマテリアルとは，少なくとも一次元の大きさが100 nm以下で製造された超微細材料と定義されている（毛髪の太さ：50 μmの1/500)。ナノマテリアルは，従来までのサブミクロンサイズ以上（100 nm以上）の素材とは異なり，サイズ減少に伴う組織浸透性の増大や電子反応性の増大，重量あたりの表面積の増加等により，有用成分の吸収性，抗酸化効果や紫外線遮蔽効果といった有用機能が格段に向上しており，われわれの生活の質的向上に革命を起こすものと期待されている[1~3]。

さらに最近では，タンパク質と同等のサイズ領域であるサブナノサイズ（10 nm以下）のナノマテリアルの開発・実用化も進んでおり，例えば，医薬品・食品・化粧品領域では，ナノサイズ・サブナノサイズのシリカや酸化チタン，フラーレン，白金，銀等がすでに，必須素材として上市されている。食品分野においては，ナノサイズに制御することによって発揮される高い吸湿性や抗菌作用，抗酸化作用を利用して，ナノシリカやナノ銀，ナノ白金等のナノマテリアルが食品添加物や機能性成分として適用されつつある。また，食品ナノマテリアルの研究開発および実用化は急速に進展しており，2008年の米国食品医薬品局（FDA）の調査では，ナノマテリアル含有食品・飲料はすでに80品目を超えていることが報告されている。

一方で，例えば強い抗菌作用はわれわれの身体を構成する細胞の機能や常在菌のバランス等にも望ましくない影響を与えてしまい得る等，ナノマテリアルの物性（サイズ，形状等）に起因した革新的機能が逆に，二面性を呈してしまい，サブミクロンサイズ以上の従来型素材では観察されない，特徴的なハザード（いわゆる，ナノ毒性；NanoTox）を発現してしまうことが世界的に懸

念され始めている。

例えば，今後の詳細な検証が必要ではあるものの，ある種のカーボンナノチューブが，アスベストと同様に悪性中皮腫を誘発する可能性が報告されている（一方で，ある種のカーボンナノチューブは安全であることもわかっている）。すなわち，分散性（二次粒径）によっても，ナノマテリアルの安全性は大きく変動するため，イントララボ間・インターラボ間でのバリデーションが重要となるうえ（この点が非常に悩ましい），同じ組成（化学構造式）でも安全性が異なることを意味しており，既存の化学物質の審査および製造などの規制に関する法律（化審法）等での規制は難しいのでは？　と言われてしまう理由でもある。そのため，経済協力開発機構（OECD）と連携しつつ，欧米各国等はナノマテリアルの安全性情報の収集を推進している。わが国でも厚生労働省や経済産業省，環境省，内閣府を中心にナノマテリアルの安全性評価研究が，今まさにスタートしたところである。

Ⅱ　安全性研究の現状

現状の安全性研究は，ナノマテリアルの腹腔内や静脈内への過剰量投与によるハザード評価が中心であり，実際の曝露実態を加味した投与量・投与経路での体内動態や細胞内動態を追求し，リスク（ハザードと曝露時間・量との積算）を解明しようとする研究は国内外を問わず，皆無に等しい。このように，実際の曝露実態を無視した一部のナノマテリアルの部分的なハザード情報が独り歩きし，闇雲な規制が施行されてしまうと，ナノマテリアルすべてが危険であるかのような風評が広がり，ナノマテリアルが社会から拒絶されかねない。ナノマテリアルを取り巻くこのような八方塞がりの状況を打開し，ナノマテリアルを活用した豊かな社会の構築と国民の健康確保を両立するためには，ナノマテリアルの曝露実態や曝露時間，体内動態情報も加味した科学的根拠に基づいた安全性情報（リスク情報）の収集が不可欠である。特に，食品は年齢・性別・健康状態を問わずすべてのヒトが一生涯にわたって摂取するため，ナノマテリアル含有食品の安全性評価は喫緊の課題の１つとなっている。

しかし，化粧品や医薬品等と比べて，食品ナノマテリアルの安全性評価は立ち遅れているのが現状であり，腸管吸収性・体内移行性に関する情報すらほとんど得られていない。体内吸収性すら明らかでない状況では，食品ナノマテリアルについてはリスク解析の必要性すら不明である。すなわち，冷静に鑑みると，食品ナノマテリアルを経口摂取しても，体内に吸収されない限り安全であり，また吸収されたとしても速やかに排泄される，あるいは蓄積せずに代謝されるのであればリスクは低いものと予想されることから，食品ナノマテリアルの吸収・分布・蓄積・排泄を詳細に評価し，今後のリスク解析の必要性の是非を，今こそ追求することが最重要課題と考えられる。

本観点から筆者らは，安全かつ有用なナノマテリアルの開発と実用化支援に資する基礎情報の収集を目指して，物性・動態・生体影響の三者連関と，曝露実態を加味した安全性評価研究によるナノマテリアルの安全科学研究（Nano-Safety Science）を推進している（図１）。特に，食品ナノマテリアルについては，リスク解析の必要性を判断するため，食品中で利用されている非晶質ナノシリカやナノ白金，ナノ銀等に関して，体内吸収性さらには体内動態情報の収集を試みており，体内に吸収される素材についてはオルガネラ移行性等をはじめとする細胞内動態を精査している。本総説では，一般的な話および経口曝露後の安全性ではないものの，先行して研究成果が蓄積されつつある経皮曝露後の安全性に焦点を絞らせていただき，特に，試薬グレードの非晶質ナノシリカの

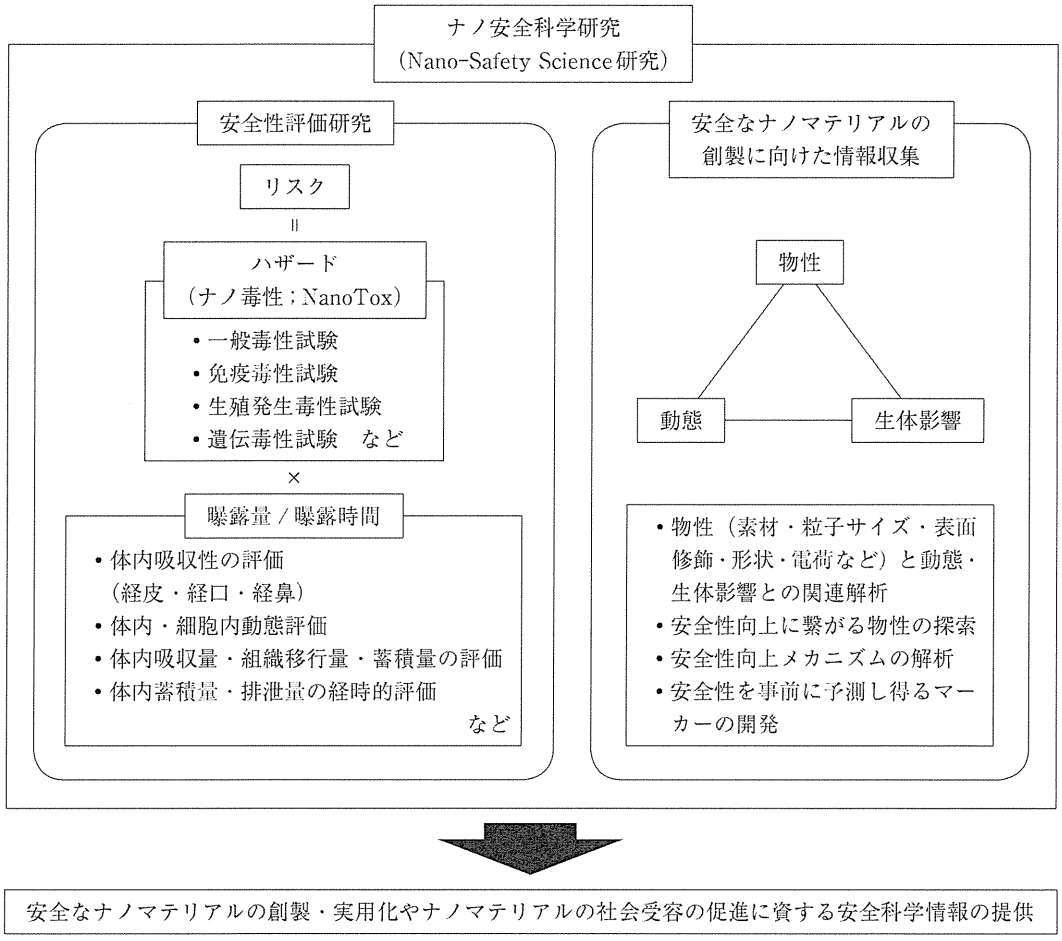

図１　ナノ安全科学研究の概略

体内動態評価を中心とした筆者らの取組みを紹介し，各方面の先生方からご意見・ご批判を仰ぎたい。

Ⅲ　非晶質ナノシリカの体内吸収性評価

数あるナノマテリアルのなかでも非晶質ナノシリカ（以下，ナノシリカ）は人体に直接適用する製品（化粧品・食品・医薬品）において最も使用量が多い素材であり，2006年の国内年間使用量はおよそ13,500トン，世界での年間生産量は1メガトンを超える[4~6]。ナノシリカの用途は非常に幅広く，日焼け止めやファンデーション等の化粧品基材，歯磨き粉や歯の充填剤，さらには食品の固結防止剤として利用されている[6]。ナノシリカは，食品衛生法により食品中に2%まで添加することが許可されているが，母乳代替食品および離乳食に使用してはならないという使用制限が規定されているのみで，その粒径や物性等に関する規定は存在していない。2009年に実施された日本食品添加物協会の調査によると，食品添加物として使用される非晶質シリカの一日摂取量は530 μgであると推定されている。また，ナノシリカは微小化や高分散化することによって，被覆